chemosensors

Supplementary Materials

Aggregation-Induced Emission-Active Iridium(III) Complexes for Sensing Picric Acid in Water

Ping He [1], Yan Chen [1], Xiao-Na Li [2], Ying-Ying Yan [1] and Chun Liu [1,*]

[1] State Key Laboratory of Fine Chemicals, Frontier Science Center for Smart Materials, School of Chemical Engineering, Dalian University of Technology, Dalian 116024, China
[2] School of Environmental Science and Technology, Key Laboratory of Industrial Ecology and Environmental Engineering (MOE), Dalian University of Technology, Liaoning 116024, China
* Correspondence: cliu@dlut.edu.cn; Tel.: +86-411-84986182

Contents

1. Phosphorescence decay curves of Ir1–Ir3

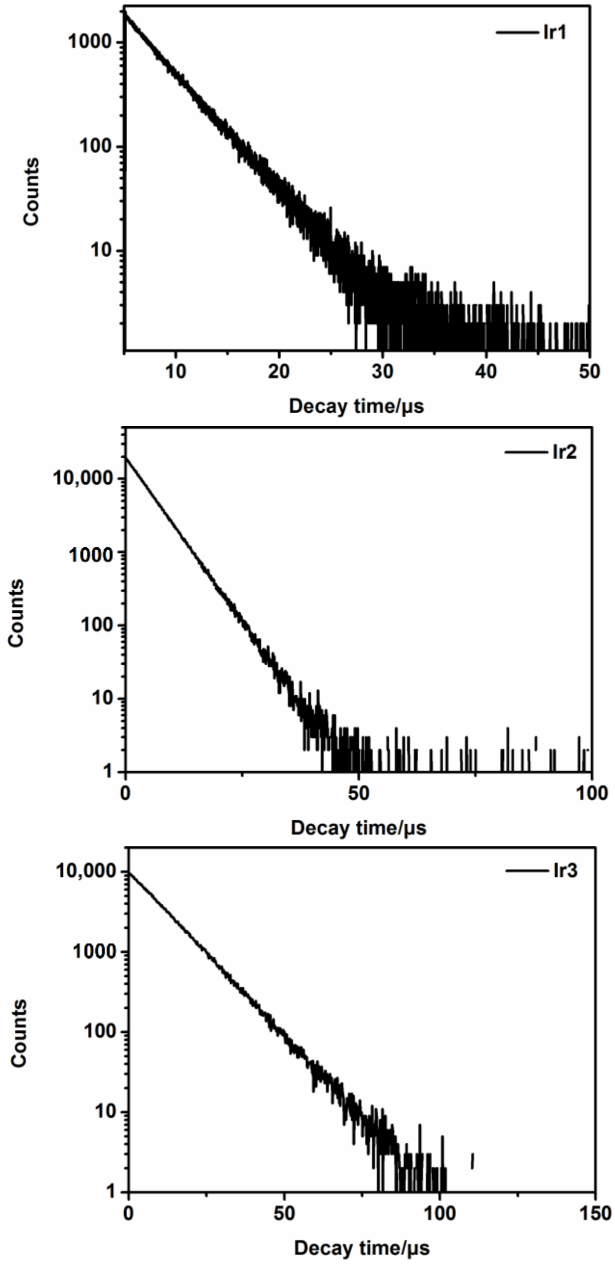

Figure S1. Phosphorescence decay curves of **Ir1–Ir3** in deoxygenated CH_2Cl_2.

2. Calculation of limits of detection (LOD) of Ir1–Ir3

The limits of detection of **Ir1**, **Ir2** and **Ir3** were calculated according to the following equation LOD = $3\sigma/K$ (σ represents the standard deviation of the blank measurement, K represents the slope of the linear regression). The limits of detection of **Ir1**, **Ir2** and **Ir3** for PA were calculated to be 50.17, 4.64, and 2.52 nM, respectively.

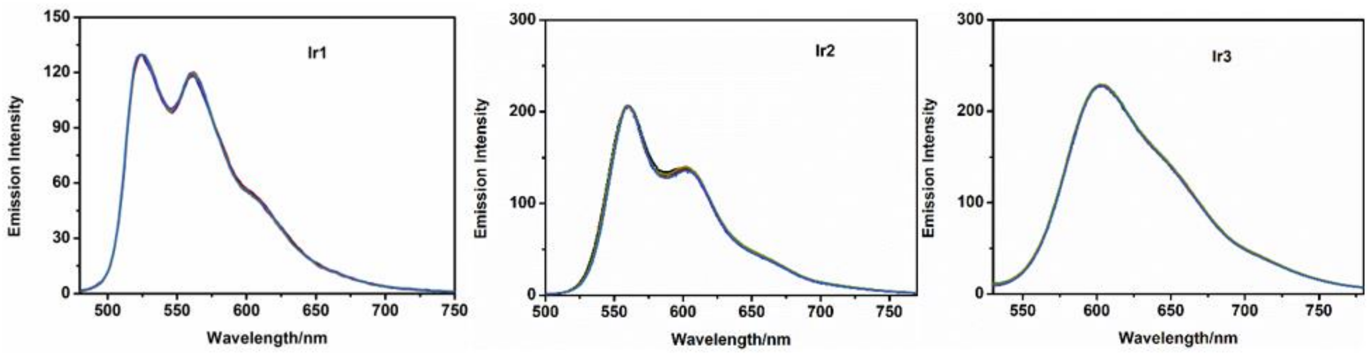

Figure S2. The emission spectra of **Ir1–Ir3** in H_2O/CH_3CN (v/v = 9:1, 10.0 μM) for eleven times (blank measurement). The excitation wavelengths of **Ir1**, **Ir2** and **Ir3** were 400 nm, 400 nm and 440 nm, respectively.

The values of *σ* for **Ir1-Ir3** were calculated according to the following equation:

$$\sigma = [\ \sum(X_i - X)^2 / (n-1)\ ]^{0.5}$$

X_i (i = 1, 2, 3…11) represents the emission intensity of each test, X represents the mean value of the emission intensity, n represent the number of tests.

Table S1. The emission intensity of **Ir1** at 525 nm, **Ir2** at 560 nm and **Ir3** at 603 nm in eleven times in H_2O/CH_3CN (*v*/*v* = 9:1, 10.0 μM).

Complex	X_1	X_2	X_3	X_4	X_5	X_6	X_7	X_8	X_9	X_{10}	X_{11}	X
Ir1	129.69	129.49	129.44	129.68	129.57	129.65	129.71	129.44	129.70	129.62	129.73	129.61
Ir2	206.63	206.51	206.74	206.46	206.43	206.59	206.60	206.65	206.32	206.52	206.54	206.55
Ir3	228.14	228.09	228.34	228.46	228.43	228.39	228.22	228.35	228.32	228.12	228.34	228.29

According to the above formula, the values of *σ* for **Ir1–Ir3** were calculated to be 0.1092, 0.1160, and 0.1282, respectively.

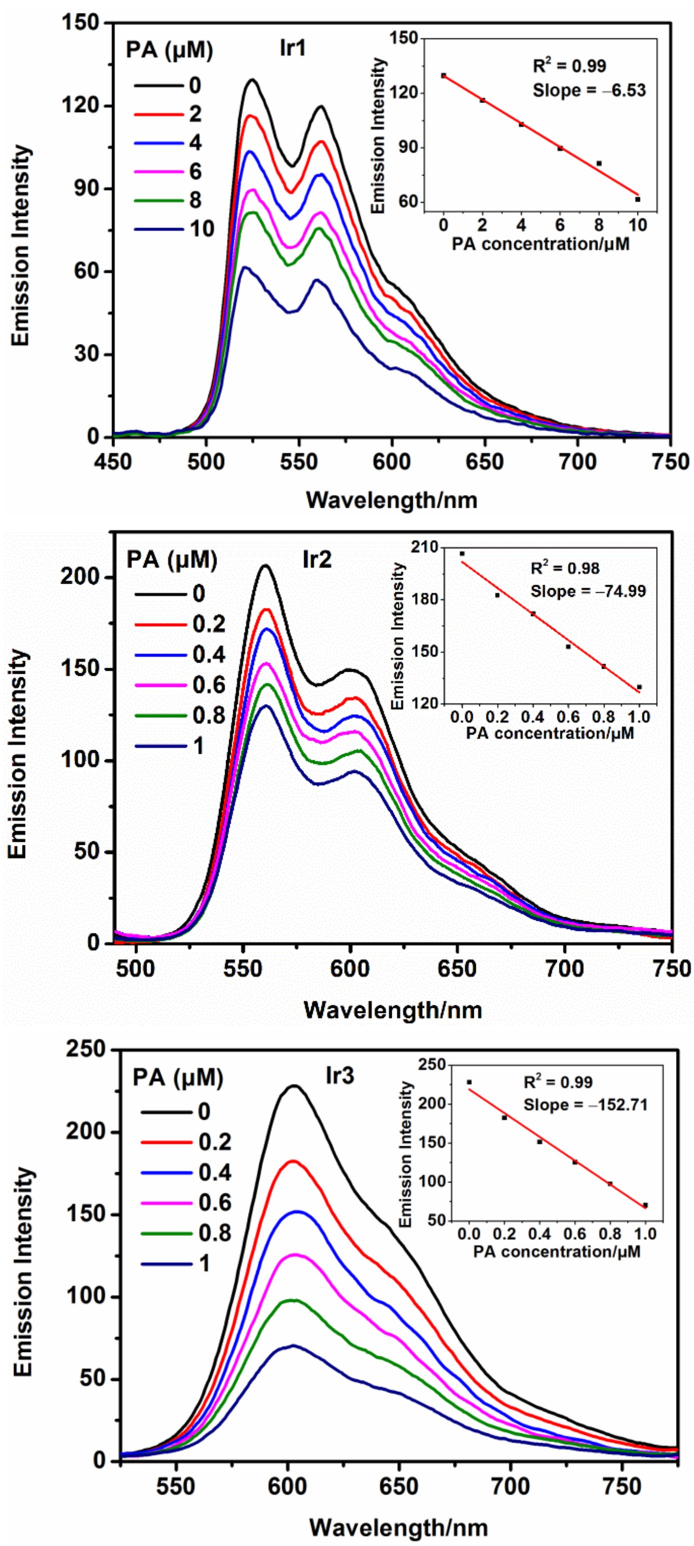

Figure S3. The emission spectra of **Ir1**, **Ir2** and **Ir3** at 10 μM after adding different concentrations of PA in H_2O/CH_3CN (*v*/*v* = 9:1). Insert: the slope of the linear regression. The excitation wavelengths of **Ir1**, **Ir2** and **Ir3** were 400 nm, 400 nm and 440 nm, respectively.

3. Previously reported PA sensors

Table S2. A comparison of solvent, K_{SV} and LOD for some sensors in detecting PA.

Ir(III) complex	Solvent	K_{SV}	LOD	Reference
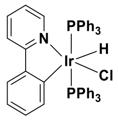	H_2O/THF (v/v = 9/1)	190000 M^{-1}	65 nM	[1]
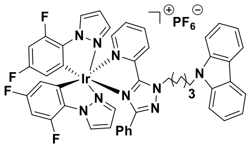	H_2O/MeCN (v/v = 9/1)	3790000 M^{-1}	10 ppb	[2]
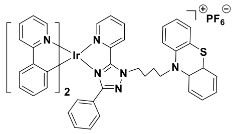	H_2O/Acetone (v/v = 9/1)	52800 M^{-1}	—	[3]
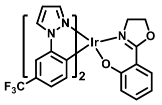	H_2O/MeCN (v/v = 9/1)	32000 M^{-1}	0.15 μM	[4]
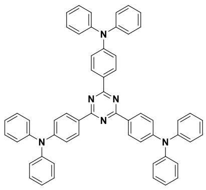	Aqueous	353000 M^{-1}	0.37 nM	[5]
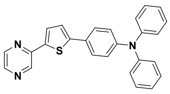	CH_2Cl_2	41338 M^{-1}	2.52 μM	[6]
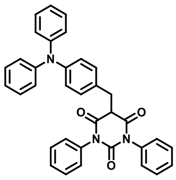	H_2O/THF (v/v = 9/1)	41000 M^{-1}	2.40 μM	[7]
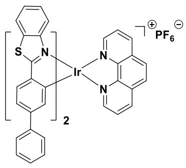	H_2O/MeCN (v/v = 9/1)	459000 M^{-1}	4.64 nM	This work
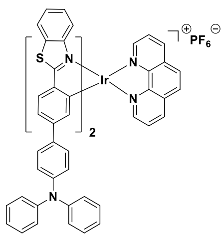	H_2O/MeCN (v/v = 9/1)	1960000 M^{-1}	2.52 nM	This work

4. The selectivity of Ir(III) complexes for detecting PA

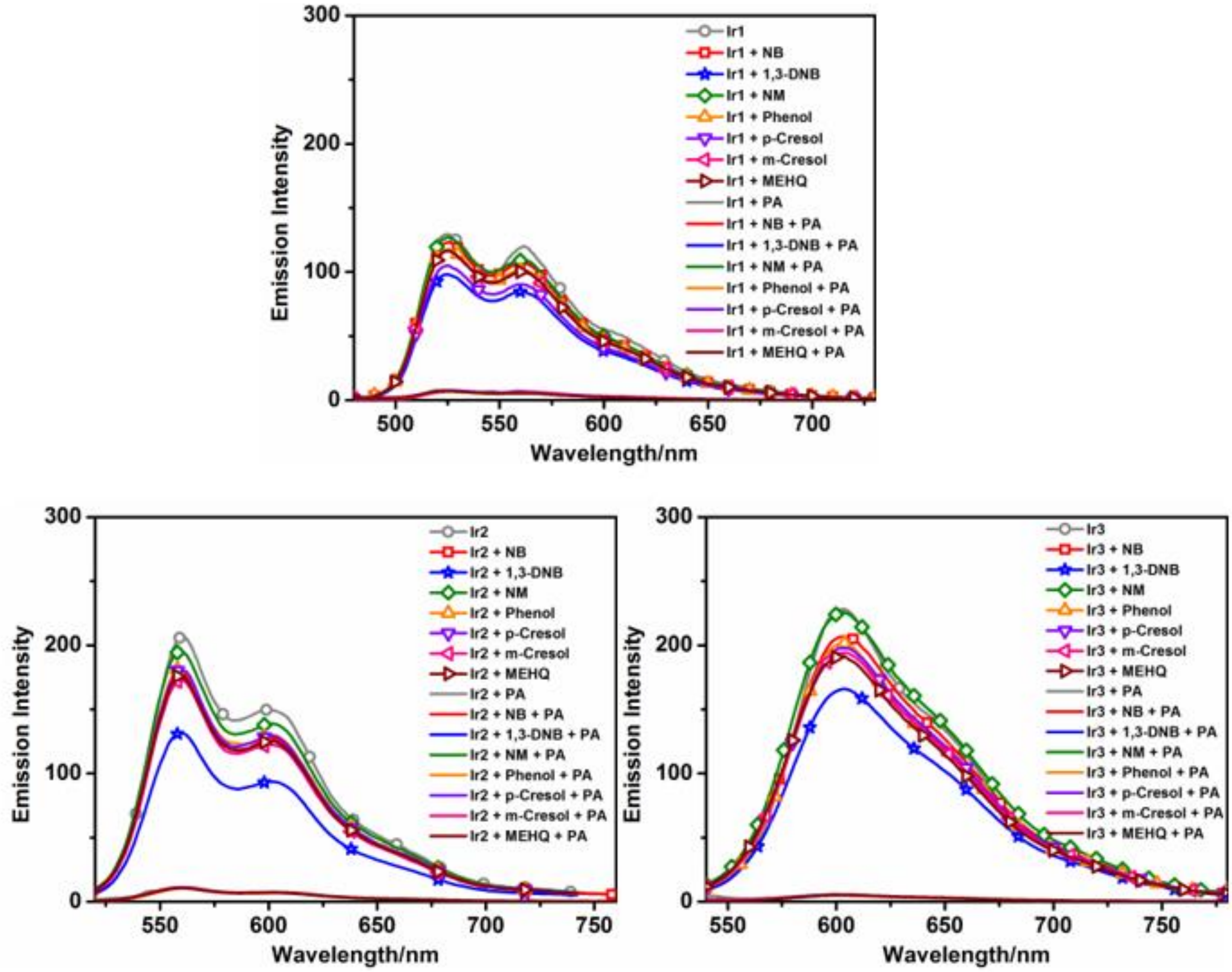

Figure S4. Emission spectra of **Ir1**–**Ir3** (10 μM) in presence of different analytes (8.0 equiv.) in H_2O/CH_3CN (v/v = 9:1). The excitation wavelengths were 400 nm, 400 nm and 440 nm, respectively.

5. [1]H NMR spectra and HRMS analysis

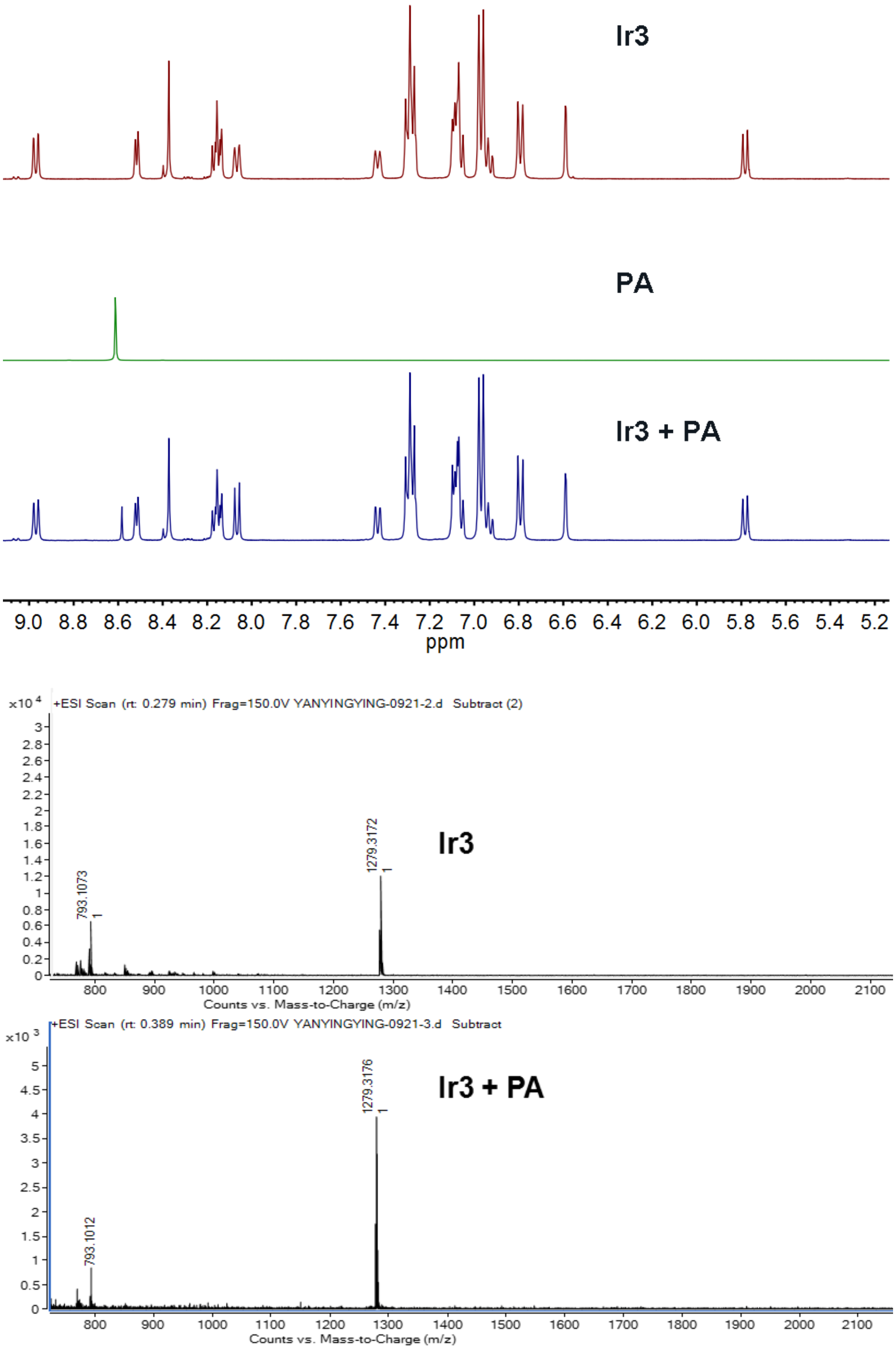

Figure S5. [1]H NMR spectra (in DMSO-d_6) and HRMS of the cationic portion of **Ir3** before and after addition of PA.

6. NMR spectra and HRMS of Ir1–Ir3

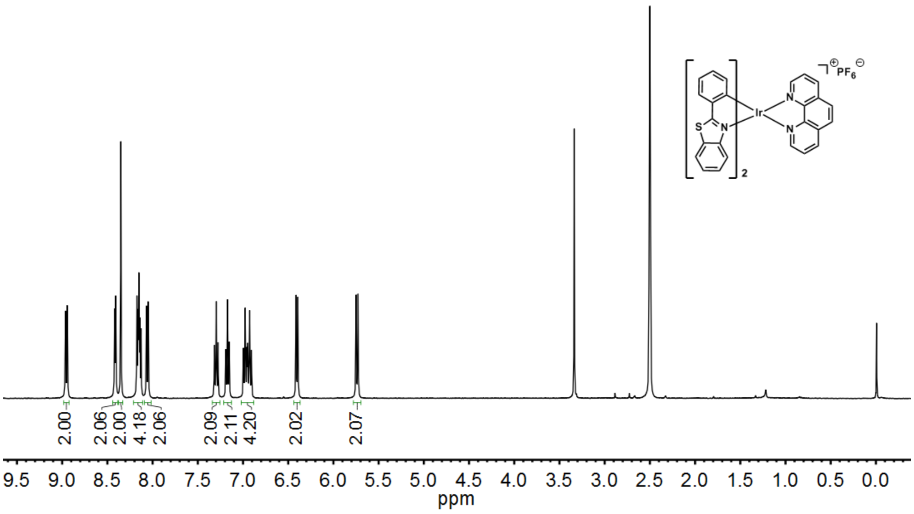

Figure S6. ^{1}H NMR spectrum of **Ir1** in DMSO-d_6.

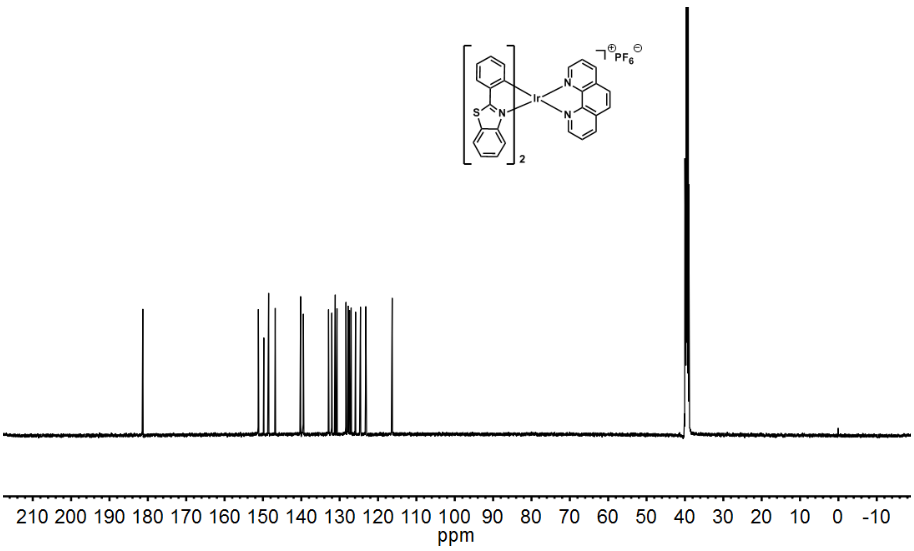

Figure S7. ^{13}C NMR spectrum of **Ir1** in DMSO-d_6.

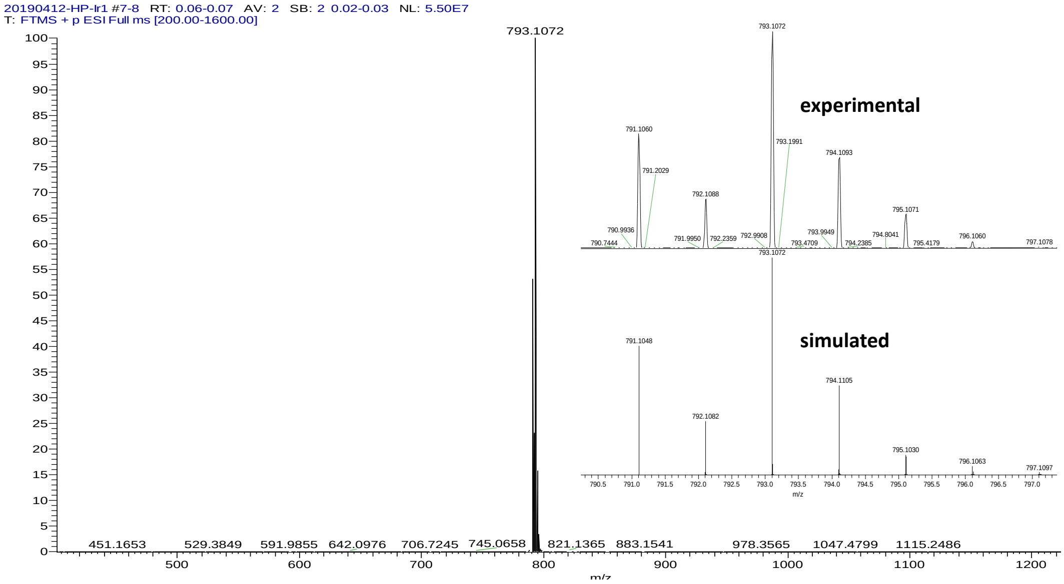

Figure S8. HRMS of the cationic portion of **Ir1**.

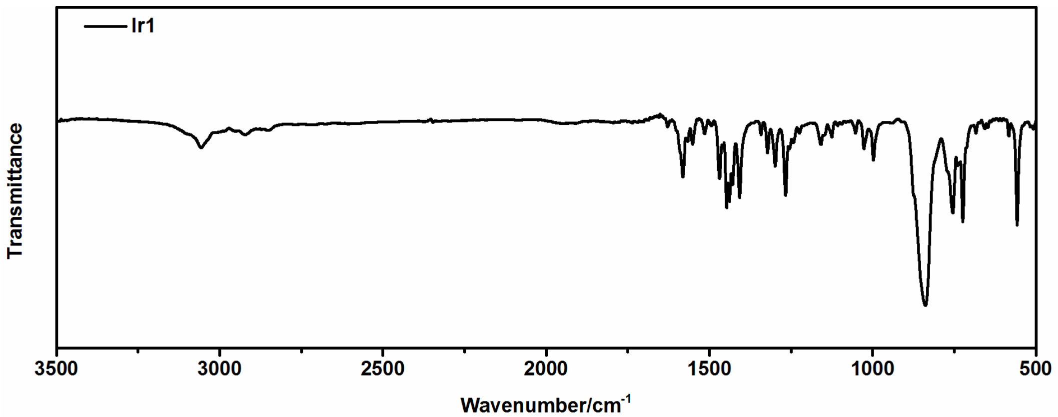

Figure S9. FT-IR spectrum of **Ir1**.

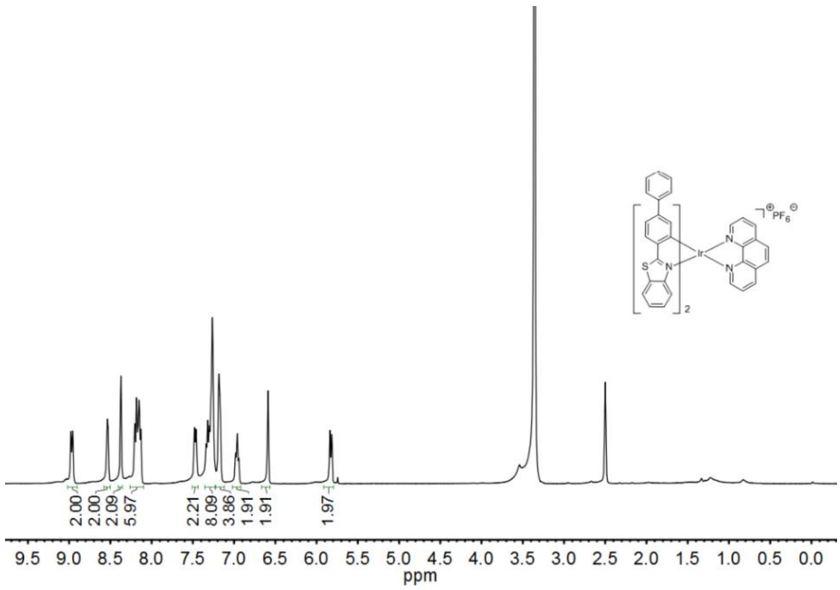

Figure S10. ^{1}H NMR spectrum of **Ir2** in DMSO-d_6.

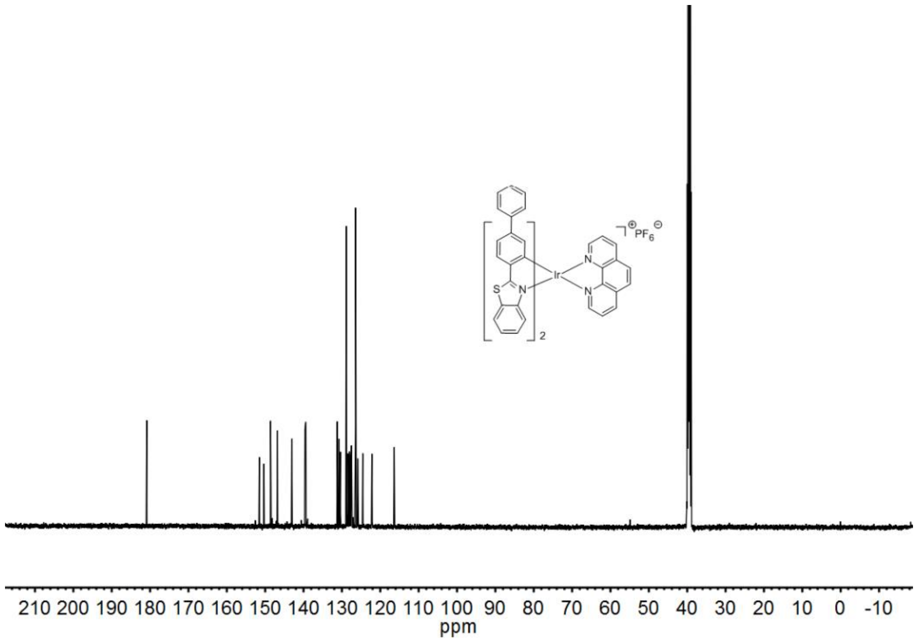

Figure S11. [13]C NMR spectrum of **Ir2** in DMSO-d_6.

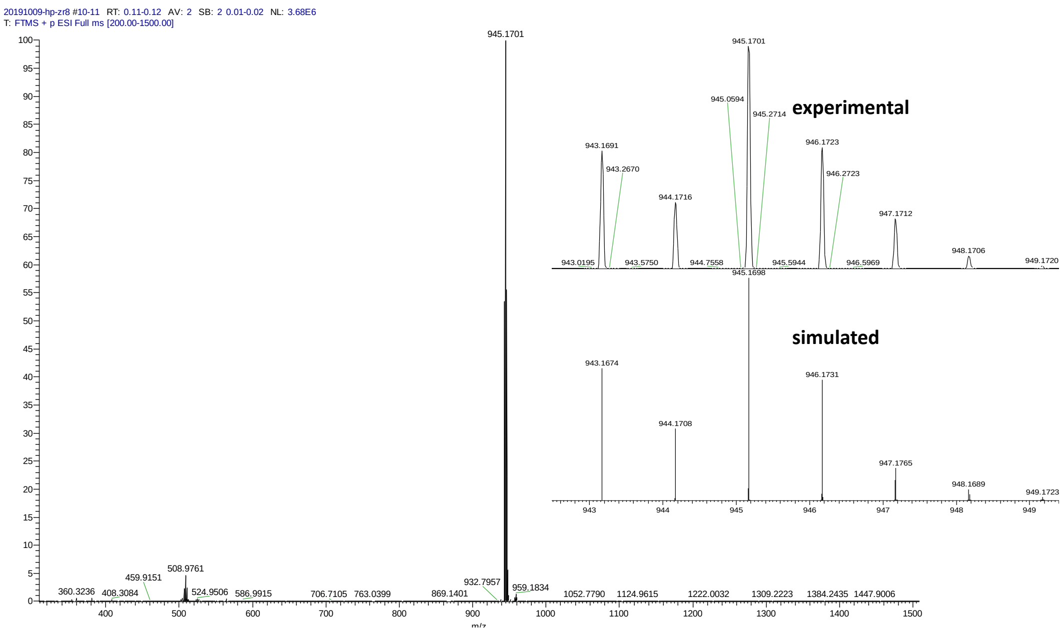

Figure S12. HRMS of cationic portion of **Ir2**.

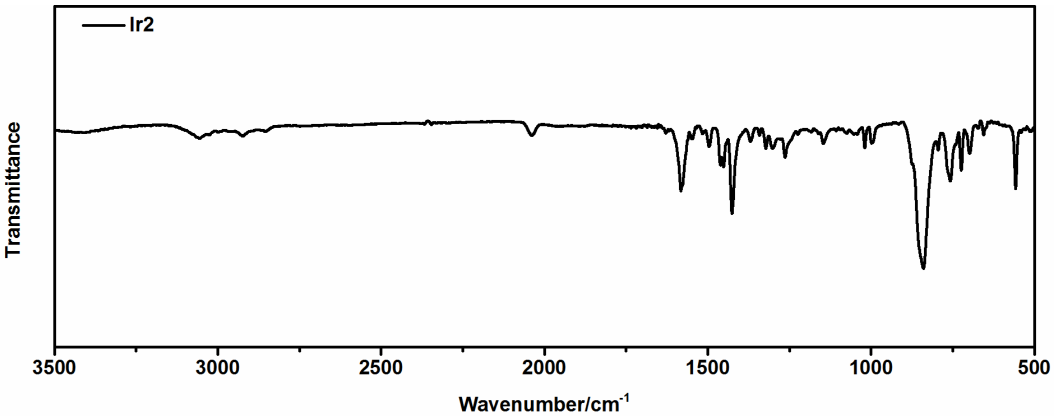

Figure S13. FT-IR spectrum of **Ir2**.

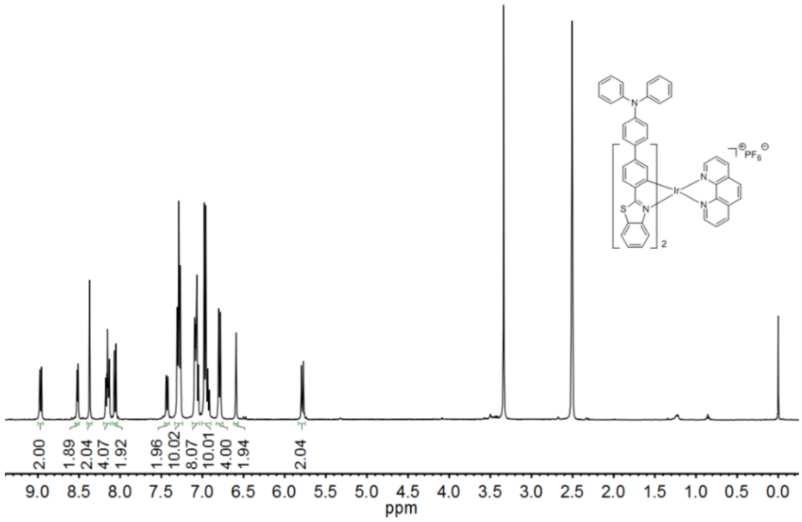

Figure S14. ^{1}H NMR spectrum of **Ir3** in DMSO-d_6.

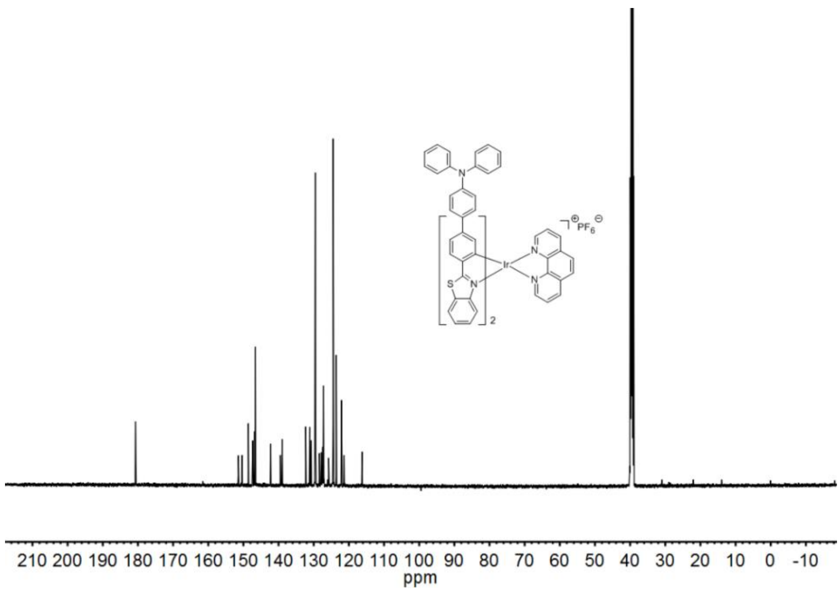

Figure S15. ^{13}C NMR spectrum of **Ir3** in DMSO-d_6.

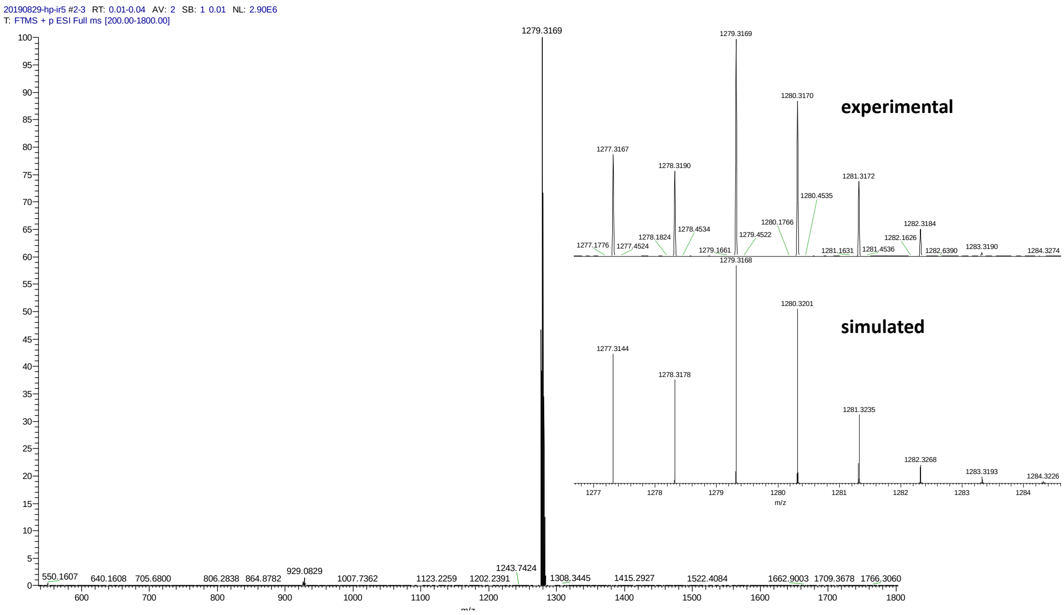

Figure S16. HRMS of cationic portion of **Ir3**.

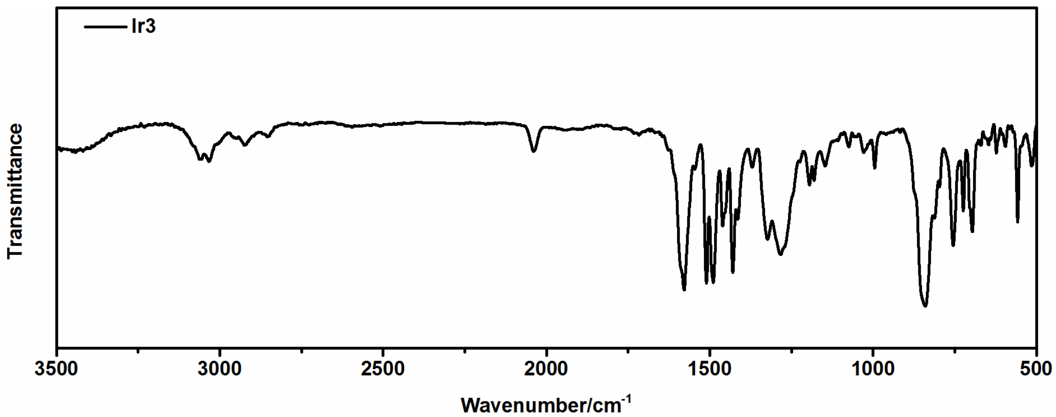

Figure S17. FT-IR spectrum of **Ir3**.

References

1. Alam, P.; Kaur, G.; Kachwal, V.; Gupta, A.; Roy Choudhury, A.; Laskar, I.R. Highly sensitive explosive sensing by "aggregation induced phosphorescence" active cyclometalated iridium(III) complexes. *J. Mater. Chem. C* **2015**, *3*, 5450–5456. https://doi.org/10.1039/C5TC00963D.
2. Wen, L.-L.; Hou, X.-G.; Shan, G.-G.; Song, W.-L.; Zhang, S.-R.; Sun, H.-Z.; Su, Z.-M. Rational molecular design of aggregation-induced emission cationic Ir(III) phosphors achieving supersensitive and selective detection of nitroaromatic explosives. *J. Mater. Chem. C* **2017**, *5*, 10847–10854. https://doi.org/10.1039/C7TC03535G.
3. Hou, X.-G.; Wu, Y.; Cao, H.-T.; Sun, H.-Z.; Li, H.-B.; Shan, G.-G.; Su, Z.-M. A cationic iridium(III) complex with aggregation-induced emission (AIE) properties for highly selective detection of explosives. *Chem. Commun.* **2014**, *50*, 6031–6034. https://doi.org/10.1039/C3CC49395D.
4. Che, W.; Li, G.; Liu, X.; Shao, K.; Zhu, D.; Su, Z.; Bryce, M.R. Selective sensing of 2,4,6-trinitrophenol (TNP) in aqueous media with "aggregation-induced emission enhancement" (AIEE)-active iridium(III) complexes. *Chem. Commun.* **2018**, *4*, 1730–1733. https://doi.org/10.1039/C7CC08832A.
5. Sathiyan, G.; Balasubramaniam, B.; Ranjan, S.; Chatterjee, S.; Sen, P.; Garg, A.; Gupta, R.; Singh, A. A novel star-shaped triazine-triphenylamine–based fluorescent chemosensor for the selective detection of picric acid. *Mater. Today Chem.* **2019**, *12*, 178–186. https://doi.org/10.1016/j.mtchem.2019.01.002.

6. Verbitskiy, E.V.; Kvashnin, Y.A.; Baranova, A.A.; Khokhlov, K.O.; Chuvashov, R.D.; Schapov, I.E.; Yakovleva, Y.A.; Zhilina, E.F.; Shchepochkin, A.V.; Makarova, N.I.; et al. Synthesis and characterization of linear 1,4-diazine-triphenylamine–based selective chemosensors for recognition of nitroaromatic compounds and aliphatic amines. *Dyes Pigm.* **2020**, *178*, 108344. https://doi.org/10.1016/j.dyepig.2020.108344.
7. Zhang, H.-J.; Tian, Y.; Tao, F.-R.; Yu, W.; You, K.-Y.; Zhou, L.-R.; Su, X.; Li, T.-D.; Cui, Y.-Z. Detection of nitroaromatics based on aggregation induced emission of barbituric acid derivatives. *Spectrochim. Acta Part A* **2019**, *222*, 117168. https://doi.org/10.1016/j.saa.2019.117168.